THERMAL DETECTORS FOR X-RAY ASTRONOMY

Stephen S. Holt

Laboratory for High Energy Astrophysics, NASA/GSFC, Greenbelt, MD, USA

ABSTRACT. Spectroscopy is traditionally characterized by the sacrifice of quantum efficiency for high spectral resolution. Since X-ray astronomy is a photon-limited discipline, the choice between high resolution for very few sources versus much lower resolution for many more has not always been an easy one. The development of new thermal detectors offers the opportunity to "have one's cake and eat it, too."

CHARACTERISITICS OF AN "IDEAL" SPECTROMETER

The most important attributes of a spectrometer depend upon the specific scientific objectives of a particular investigation, but there are some which are so generally useful that they can be safely assumed to be characteristic of an ideal spectrometer. These attributes include energy resolution sufficient to address the most important scientific objectives for all classes of sources, and simultaneous sensitivity over a wide bandpass with near-unit efficiency and negligible background. In particular, the following discussion will consider such a spectrometer for the AXAF (Advanced X-Ray Astrophysics Facility).

The primary characteristic of any spectrometer is its energy resolution, or equivalently, its resolving power:

Resolving power: $R(E) = E/FWHM(E)$

where $FWHM(E)$ is the full-width-half-maximum energy resolution at energy E, so that $R(E)$ is the X-ray energy measured in units of the resolution

Clearly, higher resolving power is "better," but it is worth examining whether or not a case can be made for a practical upper bound to the resolving power based upon purely astrophysical considerations.

A good starting place for the determination of the required resolving power derives from an examination of standard coronal equilibrium spectra in the temperature range 10^{6-8} K. Figure 1 displays such spectra for solar abundances as viewed by a detector at the focus of the AXAF telexcope with perfect efficiency over the entire bandpass. The three traces in each panel are for FWHM = 1, 10 or 100 eV.

https://doi.org/10.1017/S0252921100012562 Published online by Cambridge University Press

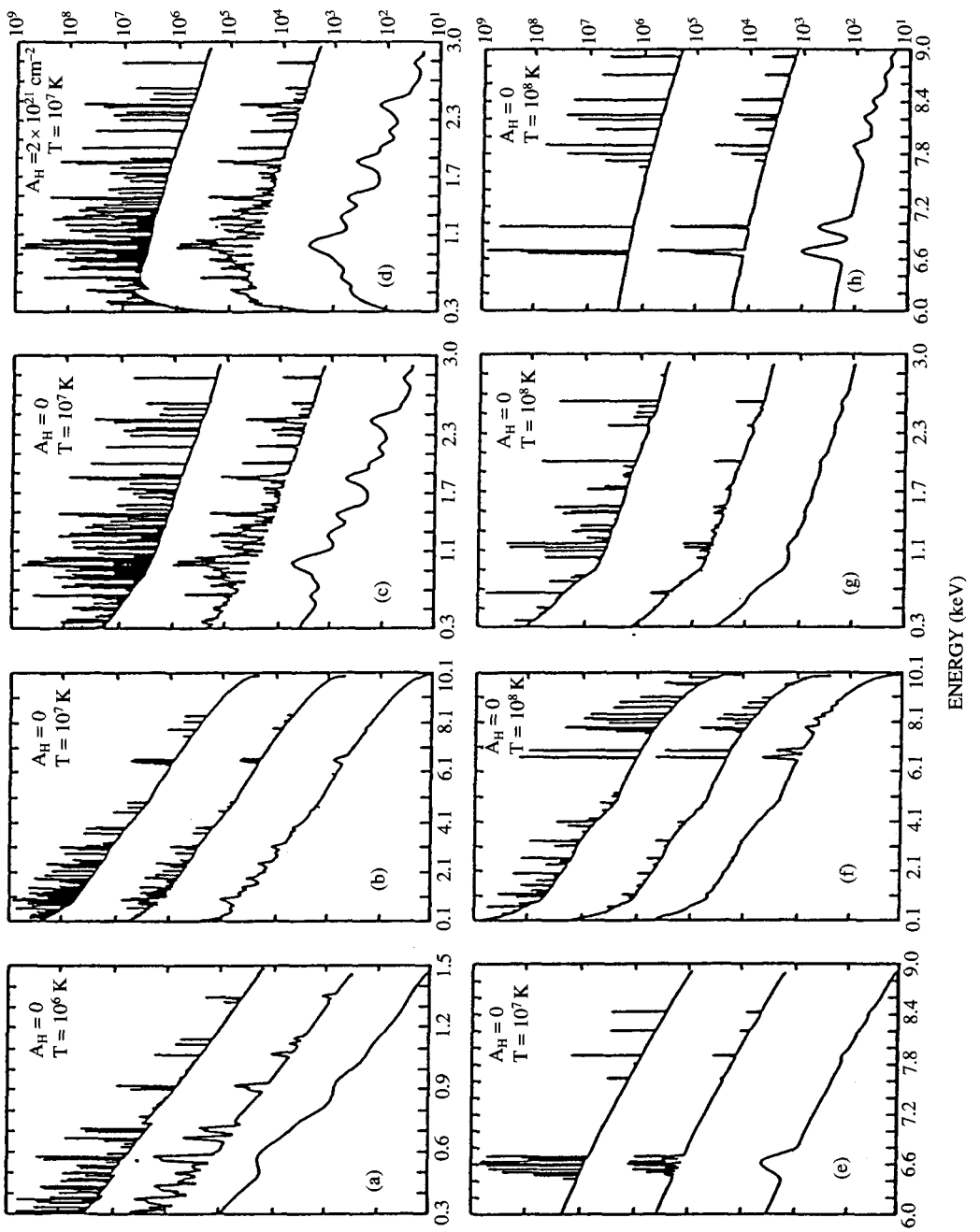

Figure 1. Coronal equilibrium spectra of plasmas with solar abundances, as viewed with detectors having FWHM resolutions of 1, 10 and 100 eV (upper, middle and lower trace of each panel).

https://doi.org/10.1017/S0252921100012562 Published online by Cambridge University Press

In general, the identification and interpretation of features that are superposed on the continuum requires increasingly better spectral resolution as the features become weaker, or as they become confused with other features from which they cannot be resolved. At temperatures near 10^8 K, an equilibrium thermal spectrum is dominated by bremsstrahlung continuum, and exhibits strong isolated Fe K-emission at energies >6.6 keV, as well as Fe L-lines near 1.2 keV. Note, however, that the "completely ionized" lower-Z elements exhibit strong recombination lines: H-like Si XIV (at 2.0 keV) and S XVI (at 2.6 keV), each with about 30 eV equivalent continuum widths, are barely discernible with FWHM 100 eV, but FWHM 10 eV can reveal O VIII at 0.65 keV and even separate Ne X and Mg XII from the Fe L-band emission. At temperatures near 10^7 K, where the power emitted in the lines and the continuum are comparable, FWHM 100 eV can separate the K-emission complexes of the abundant elements (here dominated by He-like rather than H-like analogs for Z>10), while 10 eV uncovers most of the detail that 1 eV can fully resolve. At 10^6 K, the equilibrium spectra are line-dominated; here O and Ne may be recognized with 100 eV, but FWHM 10 eV is necessary to extract quantitative information.

Atomic lines provide diagnostics for electron temperature, ionization temperature, density, mass motion and elemental abundances. The model-dependent interpretation of these diagnostics can also be used to distinguish among thermalization, shock heating or photoionization, as well as the extent to which the plasma is in the ionizing or recombining phase, so that even its history may be gleaned from its current status. The required minimum sensitivities depend, of course, on the details of the scientific problems which the observations are intended to address. The utilization of these diagnostics can be found in many references (e.g. Bahcall and Sarazin 1978; Pradhan and Shull, 1981).

For L-shell to K-shell transitions, which dominate the E > 1.3 keV spectrum of hot plasmas, the most important lines are those from:

- o the fluorescence of cold (neutral) material,
- o the analog of Lya from hydrogen-like material, and
- o the resonance (r), forbidden (f) and intercombination (i) transitions of helium-like material.

Fluorescence and Lya-analog recombination are clearly the low and high temperature limiting cases, and the helium-analog lines are important because there is a wide range of plasma conditions and temperatures for which there is substantial population of this ionization state. Here the ratio (i+f)/r can be a useful diagnostic for electron temperature, for example, while f/i and f/(i+r) are more sensitive to density. Table 1 gives very simple analytic approximations (that are good to < 10%) for the separation energies of these five lines for elements 7 < Z < 27. The energy of Lya is, of course, Z^2 times the 10.2 eV for hydrogen, so that demanding equivalent performance of a single spectrometer for all Z would require its resolution FWHM(E) to scale the same way. For a spectrometer with constant FWHM, the required value would be that for the lowest Z that is expected to be generally useful.

TABLE 1: LINE SEPARATIONS

Line pairs	Approximate energy separation (eV)
Lya - Resonance	10 Z
Resonance - Intercombination	Z
Resonance - Forbidden	2 Z
Resonance - Neutral	10 Z

Table 1 demonstrates that while about 1 eV may be required to completely resolve all the lines of potential interest from all elements, 10 eV is sufficient to separate the most important lines from oxygen, and can totally resolve them for iron. The strong dielectronic satellite lines that solar studies have identified as useful diagnostics are also typically somewhat more than 10 eV apart from the Fe XXVI and Fe XXV lines, although there is blending of fainter companions. High velocity mass motion is easily discernible with 10 eV, e.g. the broadening expected to match that for optical lines in AGN (active galactic nuclei) , which corresponds to velocities of about 5000 km s^{-1}, is $4v_{1000}Z_{10}^{2}$ eV (v_{1000} in units of 1000 km s^{-1}). The natural width of a resonance line is about $10^{-2}Z_{10}^{4}$ eV, however, so that resonance and even narrower forbidden lines have widths that cannot be measured even with 1 eV resolution. Thermal broadening at $2(T_8Z_{10}^{3})^{1/2}$ eV would also require sub-eV resolution.

It then follows that most of the important K-shell line diagnostics from O to Fe require no better than 10 eV resolution. To obtain a general capability for the measurement of thermal or natural broadening, the resolution would have to be improved by orders of magnitude. All of the above would suggest, therefore, that about 10 keV represents an important threshold for an X-ray spectrometer.

There are at least three "efficiency" parameters that each deserve separate consideration in a detailed study of scientific objectives, but which can be combined into a single parameter that has general utility.

Quantum efficiency: $\epsilon(E)$ is the efficiency with which photons of energy E incident on the detector surface are measured with resolving power R(E)

Instantaneous bandpass: $\Delta_{ins}E$ is the energy range over which the spectrometer can operate simultaneously

https://doi.org/10.1017/S0252921100012562 Published online by Cambridge University Press

Effective overall bandpass: $\Delta_{tot}E$ is the energy range over which the quantum efficiency $\epsilon(E)$ is greater than (say) 10% of its maximum value -- for a well-matched detector-telescope combination, this would be the effective band-pass of the telescope $\Delta_{tel}E$

More is better for all three parameters, but a variety of subjective arguments can be mustered to justify "required" values. It is especially important to emphasize the scientific value of having both $\Delta_{ins}E$ and $\Delta_{tot}E$ approach $\Delta_{tel}E$ in terms of discovery potential. Any spectroscopic observation performed with such a spectrometer will not just test for a narrow spectral feature at one energy that might be predicted by a model that is currently fashionable; it will simultaneously measure the spectrum throughout the entire telescope bandpass. An additional advantage of having maximally large $\Delta_{tot}E$ is in measuring the continuum: while the sensitivities to many spectral features will scale as the square root of exposure parameters, the precision with which continuum slopes can be determined scales linearly with the bandpass.

The combining "grasp" parameter Φ is meant to be the most useful possible definition of the average efficiency. It can also be considered a measure of the "speed" of the spectrometer. Φ is a function of the source spectrum and mirror response as well as the detector, i.e. if a source spectrum integrated over the total AXAF bandpass (here taken to be 0.1-10 KeV) is S ($cm^{-2}s^{-1}$), then the rate at which photons can be detected with a perfect detector at the focus of the telescope is the convolution of the telescope area as a function of energy A(E)dE (cm^2) with the source spectrum over the telescope bandpass:

$$C\ (s^{-1}) = \int_{\Delta_{tel}E} S(E')\ A(E')\ dE'$$

We define Φ as the average quantum efficiency taken simultaneously over the entire telescope bandpass:

$$\Phi = \langle\epsilon\rangle = \frac{1}{C} \int_{\Delta_{tel}E} e(E')\ S(E')\ A(E')\ dE'$$

in order that it be clearly distinguishable from the average instantaneous efficiency $\langle\epsilon(E)\rangle$ of a spectrometer over a limited bandpass $\Delta_{ins}E$ about E. for such a spectrometer:

$$\Phi = \langle\epsilon(E)\rangle \frac{\Delta_{ins}E}{\Delta_{tel}E}$$

https://doi.org/10.1017/S0252921100012562 Published online by Cambridge University Press

General requirements for the spectroscopy of a large number of sources require the ability to investigate a reasonable portion of the telescope bandpass with a respectable level of sensitivity. Simulations can be used to demonstrate that a minumum of 10^{3-4} detected photons are generally required for detailed spectral analysis. Figure 2 displays the "logN-logS" relation for extragalactic sources with slope -1.5 (e.g. Maccacaro et al. 1982) in AXAF units, i.e., the source intensity is given in units of C s^{-1} as defined in the previous paragraph for a detector with PHI=1 at the focus of the AXAF telescope. The flatter trace (with slope -0.7) is that for sources in the galaxy, including binary accretors and supernova remnants.

The "weak source" limit of a spectrometer will be determined by the detector background B(E) in addition to Φ. As a practical matter, the acceptable background is a function of Φ; if the total detector background is a small fraction of the expected source counts, then it is effectively trivial. For a detector with Φ approaching unity, for example, there will be thousands of sources for which C > 1 ct s^{-1}, so that B(E) as high as 10^{-2} might be acceptable.

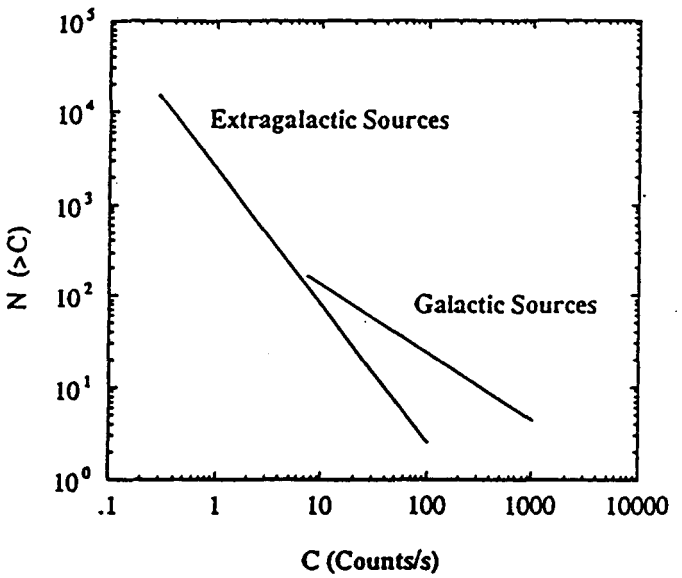

Figure 2. The number of observable sources as a function of the count rate of a perfect detector in the focal plane of AXAF.

https://doi.org/10.1017/S0252921100012562 Published online by Cambridge University Press

A totally objective (albeit incomplete) measure of the capability of a spectrometer is its sensitivity to the equivalent continuum width (EW) of a single narrow spectral feature. If the feature is narrower than FWHM(E), the detectable EW will scale as the inverse square root of the following parameters for any spectrometer:

- o the source strength,
- o the exposure time, and
- o the detector parameters $\epsilon(E)$ and $R(E)$.

For a scanning spectrometer, the same formalism may be used if $\epsilon(E)$ is the mean efficiency to the feature over the entire energy range that must be scanned during the exposure time. Additionally, the effect of background (either non-X-ray or X-rays multiplexed from other energies) on the detectable EW can be approximated with a multiplicative factor containing the ratio of the background counts B' to the source counts S' recorded within FWHM: $(1 + B'/S')^{1/2}$.

Two other parameters that can be important in determining the utility of instruments for astronomical spectroscopy are associated with angular sizes: the total instantaneous field-of-view FOV and the differential pixel size $d\Omega$ within FOV. For maximum generality, it would be nice to have FOV as large as the 30 arc min that characterizes the AXAF telescope, itself, and $d\Omega$ similarly matched to the AXAF sub-arc second spatial resolution. For purposes of estimating minimum requirements, however, the great majority of the sources in Figure 2 are point sources (i.e. not resolved by the telescope at a level < 1 arc sec), but there are important exceptions. Both supernova remnants (SNR) and clusters of galaxies are extended sources. Young SNR in our galaxy have typical sizes of arc minutes, and those in nearby galaxies are (of course) even smaller. Similarly, the core radii of bright clusters of galaxies have typical values of the order of an arc minute. It is clear, therefore, that about 1 arc minute is the minimum FOV necessary to obtain exposures that simultaneously cover large portions of the extended areas of X-ray emission in most SNR and clusters of galaxies.

From Figure 2, it is clear that there is no point source confusion problem for FOV of order 1 arc minute at 10^4 s, even for a detector with Φ=1. The important issue for $d\Omega$ is, therefore, the extent to which gradients can be measured across the same extended sources discussed in the last paragraph. There is important differential spectral-spatial information to be obtained from both SNR and clusters, e.g. cooling flows near the center in the latter, and non-equilibrium effects inside the blast wave in the former. Since the timescales for variability in these objects are longer than the lifetime of AXAF, spectral-spatial mapping with a "fast" detector could be performed in a raster mode, but the observatory would be utilized more efficiently if the whole spectal-spatial correlation was performed in a single exposure.

https://doi.org/10.1017/S0252921100012562 Published online by Cambridge University Press

A practical limit for $d\Omega$ can be obtained from the source catalog itself. For a given $d\Omega$ and FOV, we can estimate how strong an extended source would have to be in order to meet the two conditions that there were enough counts accumulated in each pixel for independent spectroscopy, and that the accumulation time was short enough to allow many different such exposures in the observing timeline. For $d\Omega$ of about an arc sec over an arc min FOV, for example, it would take a source as intense as the Crab nebula to allow a perfect focal plane detector to accumulate 10^3 counts per pixel in 10^4 s. This means that there are very few areas of extended X-ray emission for which a $d\Omega$ as small as 1 arc sec can be justified with the AXAF telescope.

CHARACTERISTICS OF AN X-RAY CALORIMETER

An X-ray calorimeter works by converting the energy of a single X-ray photon entirely into heat. For it to function as a spectrometer for individual X-rays, the effective noise in the temperature measurement must be small compared to that temperature rise.

A practical device consists of an X-ray absorber and a thermometer mounted on a substrate with small heat capacity C_0, connected by a weak thermal link of conductance G_0 to a heat sink at temperature T_0 (see Figure 3). When an X-ray of energy E is absorbed, the temperature of the substrate is increased by an amount $\Delta T = E/C_0$ in a time short compared to the time constant $\tau = C_0/G_0$ associated with recovery of the substrate back to the bath temperature T_0. The random transfer of energy between the substrate and heat sink produces fluctuations in the energy content of the substrate.

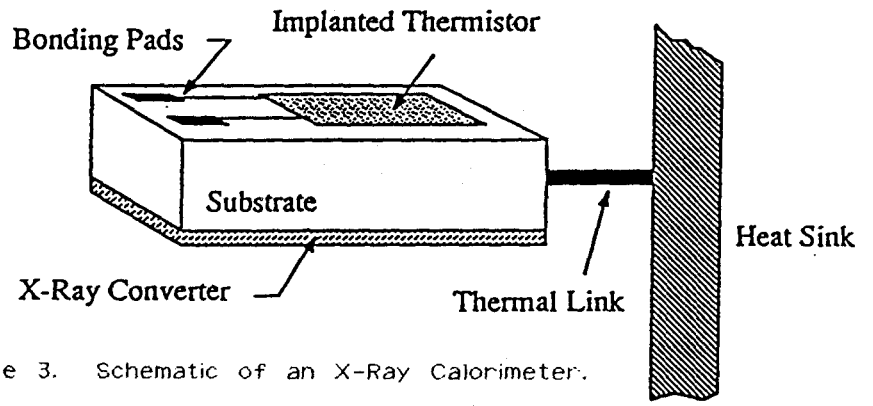

Figure 3. Schematic of an X-Ray Calorimeter.

https://doi.org/10.1017/S0252921100012562 Published online by Cambridge University Press

An elementary statistical calculation gives the mean square magnitude of these fluctuations as:

$$\langle \Delta E \rangle_{rms}\ (FWHM) = 2.35[kT_0^2 C_0]^{1/2}$$

where k is Boltzmann's constant. Note that this is independent of G_0 and any details of the thermal link. These fluctuations can be thought of as square-root N variations in the number of phonons contained in the substrate, and represent the background noise level against which the increase in energy due to an absorbed signal event must be measured. The advantages of low temperature operation are obvious, particularly when consideration is given to the fact that C_0 scales as T_0^3 with the proper choice of materials. As an example, a piece of silicon 0.5 mm on a side and 25 μm thick with heat capacity 4×10^{-15} J K^{-1} at 100 mK would have a limiting fluctuation noise of about $\Delta E_{rms} = 0.2$ eV.

The most important additional noise sources are those which might arise from the conversion of X-ray energy to heat (e.g. if some energy is trapped in states that are long-lived compared to the rise time of the heat pulse), and from the measurement of the temperature. Conversion noise may be made arbitrarily small, but the Johnson noise in ion-implanted thermistors provides an unavoidable increase in the minimum system noise achievable for this thermometry technique, as demonstrated in the seminal work of Moseley, Mather and McCammon (1984) on this subject, based on analyses of noise sources in infra-red bolometers (Mather, 1982; Mather, 1984). These authors demonstrate that in the case where only Johnson noise is an important addition, the expression for achievable noise can be approximated with a multiplicative factor ξ (with a value of about 2 for well-chosen thermistor parameters) to that for the basic fluctuations:

$$\Delta E_{rms}\ (FWHM) = 2.35\xi[kT_0^2 C_0]^{1/2}$$

An equivalent circuit for the calorimeter consists of a voltage source V_{bias} in series with both a fixed load resistor R_L and a thermistor R (across which the signal equivalent to the heat depostition Q is measured), so that $V_R = V_{bias} R/(R+R_L)$. The temperature dependence of the thermistor is given by a $\alpha = -d(\log R)/d(\log T)$, which has a typical value of 6. From the definitions of α and C_0:

$$\frac{dR}{R} = \frac{-\alpha dT}{T} = \frac{-\alpha dQ}{C_0 T} \quad \text{so} \quad \frac{dV}{dQ} = \frac{\alpha V_{bias} R R_L}{C_0 T (R+R_L)^2}$$

The responsivity S (volts/watt), essentially dV/dQ multipled by the effective recovery time τ, should increase linearly with V_{bias}, but is found instead to reach a maximum value and then decrease. One reason for this limitation is the self-heating of the thermistor increasing its heat capacity, but there are a variety of other non-ideal effects that limit the achievable responsivity.

https://doi.org/10.1017/S0252921100012562 Published online by Cambridge University Press

In order to keep the heat capacity down, especially when considering the additional components arising from the X-ray absorber and the electical connections to the thermistor, the detector sizes are limited to < 1 mm^2. For reasons originally associated with *a priori* pointing limitations that prevented AXAF from guaranteeing that a point source image could be located on such a small detector, we have baselined a 6x6 array of calorimeters in the focal plane that each operate as independent spectrometers. In addition to enlarging its FOV, this arrangment also provides some imaging capability to the spectrometer.

The small detector volumes assure that even without active anticoincidence the non-X-ray background will be small. Scaling by the relative volumes from solid state detectors that have been flown before, the backgound summed over the entire array of detector should be of order 10^{-3} s^{-1} over the entire 10 keV bandpass. Recalling from Figure 2 that there are thousands of sources that will provide count rates in excess of 1 s^{-1} for a detector as efficient as a calorimeter, this background should be negligible.

The detector efficiency is limited at low energies by the windows that must be placed between the cold detector and the thermal noise that direct radiation from warmer surroundings would produce. The current AXAF design, based upon windows that have already been tested under launch conditions, results in efficiency that rises rapidly above about 10% at 0.3 keV to a value that is prevented from reaching unity if meshes are required to maintain the integrity of the windows.

SUMMARY

The X-ray calorimeter for AXAF is still under development, but test results suggest asymptotic values for relevant spectroscopic parameters. Recent development work, including practical limitations of thermistor-implanted X-ray calorimeters and associated cryogenic systems, can be found in McCammon et al (1987), Moseley, et al (1988) and Kelley et al. (1988), and will not be discussed here. With respect to energy resolution, the current "best" value obtained in a single test is 17 eV FWHM at 100 mK, but the values for each of the contributing noise components have each been separately measured in other tests to be less than 10 eV -- this suggests that the limiting value for AXAF will certainly be better than 10 eV.

TABLE 2: SUMMARY OF EXPECTED AXAF CALORIMETER PARAMETERS

FWHM	< 10 eV
R_{max}	10^3
$\Delta_{tot}E$	0.3-10 keV
$\Delta_{ins}E$	0.3-10 keV
$\Phi=<\epsilon(E)>$	> .6
Background	effectively zero
FOV	1 arc min
$d\Omega$	10 arc sec

https://doi.org/10.1017/S0252921100012562 Published online by Cambridge University Press

A rough comparison of the expected AXAF calorimeter values for two of these parameters (R_{max} and Φ) with those from spectrometers that were flown onboard the Einstein observatory is displayed in Figure 4. Note that the effects of the larger area and increased bandpass of the AXAF telescope are not represented in this figure -- one that could properly include them would make this comparison even more striking.

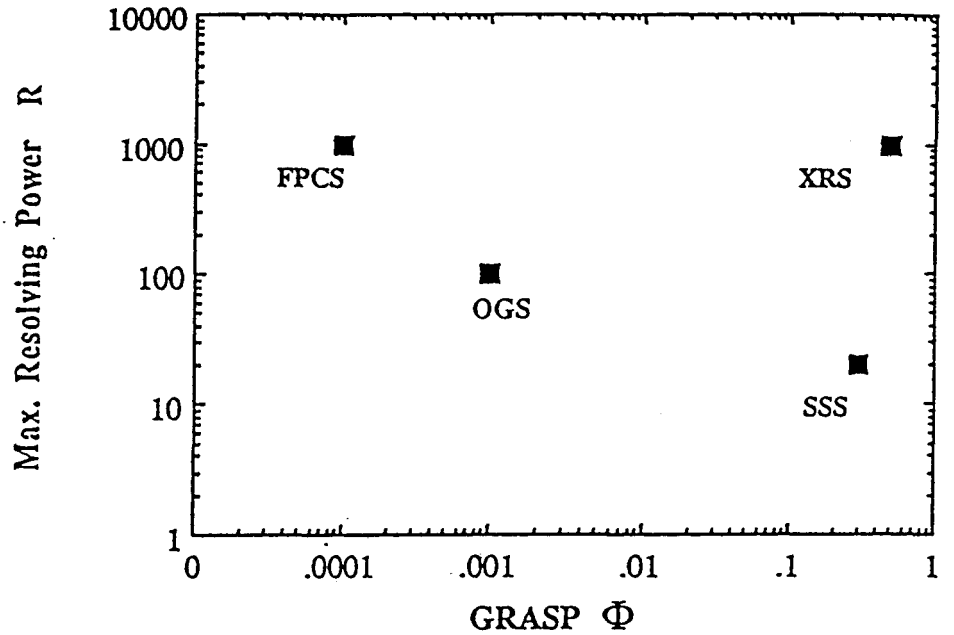

Figure 4. Comparison of maximum resolving power and grasp of the Einstein Observatory spectrometers with the AXAF calorimeter (XRS).

Observing a point source with milli-Crab intensity and an AGN-type spectrum (alpha=0.7, $N_H=10^{21}$ H-atoms/cm^2) for 10^4 s, the calorimeter described here can detect features at "interesting" energies with the following equivalent continuum widths (EW) at 99% confidence:

TABLE 3: LINE DETECTABILITY IN 10^4 S FOR A MILLICRAB SOURCE

E =	0.6 keV	Oxygen	EW = 0.5 eV
	2	Silicon	2
	7	Iron	21

Because the scaling laws go like the square roots of parameters, the formal sensitivities are not all that much better for slightly better $\epsilon(E)$ or FHWM; it is only in comparison with dispersive spectrometers that the sensitivity differences are truly dramatic.

https://doi.org/10.1017/S0252921100012562 Published online by Cambridge University Press